Journal of Geochemical Exploration 101 (2009) 247–253

Contents lists available at ScienceDirect

Journal of Geochemical Exploration

journal homepage: www.elsevier.com/locate/jgeoexp

TEM observation of geogas-carried particles from the Changkeng concealed gold deposit, Guangdong Province, South China

Jianjin Cao [a,b,*], Ruizhong Hu [b], Zhirong Liang [a], Zhuolun Peng [a]

[a] Department of Earth Sciences, Sun Yat-sen University, Guangzhou 510275, China
[b] State Key Laboratory of Ore Deposit Geochemistry, Institute of Geochemistry, Chinese Academy of Sciences, Guiyang 550002, China

ARTICLE INFO

Article history:
Received 13 November 2007
Accepted 4 September 2008
Available online 7 October 2008

Keywords:
Particles
Concealed deposit
Geogas
Origin
Implications

ABSTRACT

Geogas prospecting is a relatively new technique in exploration for deep-seated and concealed mineral deposits. Now, the technique is to reveal the presence of concealed ore bodies by analyzing the element concentrations of substances that are transported by geogas from concealed ore bodies to the Earth's surface. However, the element concentrations provide us with limited information about the concealed ore bodies. In our work, to investigate the category, size, shape, chemical component of geogas particles, copper grids for transmission electron microscopy measurement were directly used to capture the geogas-carried solid particles in Quaternary sediments overlying the Changkeng concealed gold deposit, Guangdong Province, South China. In the samples, we found Au, $PbSO_4$, WO_3, Fe_2O_3, SiO_2, TiO_2, and Al_2O_3 particles, etc. using a transmission electron microscopy. Of which, gold particles, and Hg-, Zn-, Pb-, W-bearing particles may originate from concealed ore bodies and can provide more direct information than those provided by element concentrations.

1. Introduction

Geogas prospecting is a relatively new technique in exploration for deep-seated and concealed mineral deposits that was jointly developed in the early 1980s by the Swedish mining and smelting company Boliden AB and the Department of Nuclear Physics, LTH, Lund University, Sweden (Kristiansson and Malmqvist, 1980). It can be used to explore for deposits at depths ranging from several hundred meters to 1 km below the surface. Geogas is defined as an ascending flow of gaseous matter such as N_2, O_2, CO_2, CO, CH_4, NH_3 (Tong and Li, 1999) originating from degassing of the upper mantle and lithosphere (Gold and Soter, 1980; Morner and Etiope 2002; Annunziatellis et al., 2003), releasing from ore mineral weathering (Wang et al., 2007), atmosphere driven by barometric pumping (Cameron et al., 2004). Geogas might be a global phenomenon, because it has been widely reported from many ore deposits worldwide (Xie et al., 1999). It can carry solid substances from concealed ore bodies or other geological bodies and transport them to the Earth's surface (Wang et al., 1997, 2007). Concealed ore bodies may be detected by capturing these geogas-carried substances in Quaternary sediments, and analyzing their extremely low element concentrations by instrumental neutron activation analysis (INAA), atomic absorption spectrometry (AAS), and particle induced X-ray emission (PIXE) (Kristiansson and Malmqvist, 1982, 1987; Malmqvist and Kristiansson, 1984; Kristiansson et al., 1990; Wang et al., 1997; Tong et al., 1998; Hirner, 1998; Xie et al., 1999; Malmqvist et al., 1999; Cao et al., 2004). However, the traditional methods for estimating the concealed ore bodies consist only of measuring the element concentrations of the geogas-carried particles using different analytical methods. In our work, to investigate the origin of geogas-carried particles TEM (Transmission Electron Microscopy) copper grids were directly placed in Quaternary sediments overlying concealed ore bodies to collect particles in ascending geogas. Using TEM, we measured the particle characteristics (the category, size, shape, chemical component and association) and discussed origin of the geogas particles.

2. Geological setting

Changkeng deposit in the Jinli town, Gaoyao City, Guangdong Province of southern China is located in the northwest margin of the Sanzhou Upper Palaeozoic faulted basin in the central Guangdong depression of the South China fold system, which hosts a large Carlin disseminated type gold deposit and a super large carbonate-hosted replacement-type silver deposit, and is a new type of deposit discovered in China in recent 20 years (Du et al., 1993, Zhang et al., 1997). Not any kind of igneous rocks has been found in the ore district (Sun et al., 2003). The exposed strata in the Changkeng area are Lower Carboniferous, Upper Triassic rocks and Quaternary sediments (Fig. 1). Lower Carboniferous Shidenzi Formation is mainly limestone and silty shale is fragmentary. Lower Carboniferous Ceshui Formation is stone, siltstone

* Corresponding author. Department of Earth Sciences, Sun Yat-sen University, Guangzhou 510275, China.
E-mail address: eescjj@mail.sysu.edu.cn (J. Cao).

0375-6742/$ – see front matter © 2008 Elsevier B.V. All rights reserved.
doi:10.1016/j.gexplo.2008.09.001

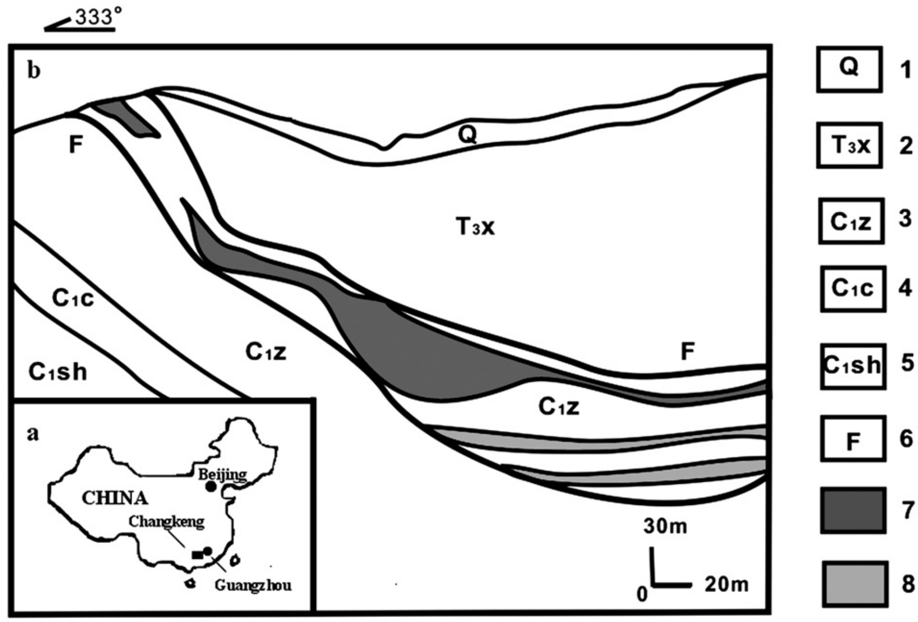

Fig. 1. Cross-section of Changkeng gold deposit (after Du et al., 1993). 1—Quaternary sediments; 2—Upper Triassic Xiaoping fm.; 3—Lower Carboniferous Zimenqiao fm.; 4—Lower Carboniferous Ceshui fm.; 5—Lower Carboniferous Shidenz fm.; 6—fault; 7—gold ore body; 8—silver ore body.

and limestone. Lower Carboniferous Zimenqiao Formation is bioclastic limestone and muddy limestone. The Upper Triassic Xiaoping Formation is sandstone, arkosic quartz sandstone, siltstone, and carbonaceous mudstone. Upper Triassic clastic rocks rest fault-unconformably on the Carboniferous Formations (Du et al., 1993). Quaternary slope sediments and alluvium widely distribute in the ore field. The concealed ore bodies are fault-controlled. The Au ore bodies are hosted in the brecciated siliceous rocks on the top of the Zimenqiao Formation bioclastic limestone. The Ag orebodies are located in the fractures in the Zimenqiao Formation bioclastic limestone (Du et al., 1993). The main two ore types are oxidation ore body and original ore body. The minerals in the oxidation ore body comprise quartz, illite, kaolinite, limolite, scorodite, magnetite, zircon, pyrite, native gold and other sulfides. Ore minerals in original gold ore bodies consist of pyrite, realgar, orpiment, antimonite, marcasite, cinnabar, arsenopyrite, and sphalerite. Their gangue minerals are quartz, calcite, barite, illite, dickite, fluorite, and gypsum. Ore minerals in original silver ore bodies consist of galena, sphalerite, freibergite, pyrargyrite, polybasite, andorite, miargyrite, argentite, cinnabar, and pyrite. Their gangue minerals are quartz, calcite, illite, fluorite, and kaolinite (Mao et al., 2007). Gold ore textures are brecciated and disseminated. The majority of the Au (>82%) occurs in native form. Minerals that carried this gold are quartz, illite, dickite, and pyrite. The native gold is distributed in microfractures of pyrite and quartz, or along the crystal rims of illite, dickite, pyrite, and quartz crystals. Alteration associated with the Au-mineralization is mainly silicification, decalcification, and argillization. The silver ore bodies are located 20–50 m down-section from gold ore bodies (Du et al., 1993; Liang et al., 2007).

3. Sampling and analytical method

The geogas particle collector consists of an ordinary plastic funnel equipped with a carbon-coated copper TEM grid (Fig. 2). The collectors were placed at a depth of 60–80 cm holes in soils. The plastic funnels were inverted to collect gas flow. TEM grids pressed from both nylon nets were placed just outside the end of the funnel spouts to capture the geogas-carried solid particles and protected by plastic cups to prevent contamination from the outside. After 45 days, the collectors were opened. The grids were taken up with fine pincers and put into TEM sample cell at once, which will put into a plastic seal box. The nylon nets, fine pincers, sample cell, seal box, plastic cups and funnels were clean with distilled water at first, washed with neutral detergent then, washed with high-purity water for several times again, dried for future use at last. Before carbon-coated copper grids were used, a blank check of 20% grids had been performed using TEM. Fourteen sites were sampled in an area of approximately 0.25 km^2. Each sampling cell was approximately 100 m × 350 m. Of which: Two TEM grids were put in the same collector in eight sampling sites, to test the repeatability of the experimental result. In barren area, geogas particle samples were collected using TEM grids for blank contrast analysis.

The geogas particle samples were analyzed using a transmission electron microscope (JEM-2010HR, JEOL LTD, Japan) equipped with an energy dispersive spectroscope (Energy TEM 200, OXFORD-INCA) at an accelerating voltage of 200 kV, which were carried out at the Instrument Analysis Center of Sun Yat-sen University. In the ore district, Quaternary

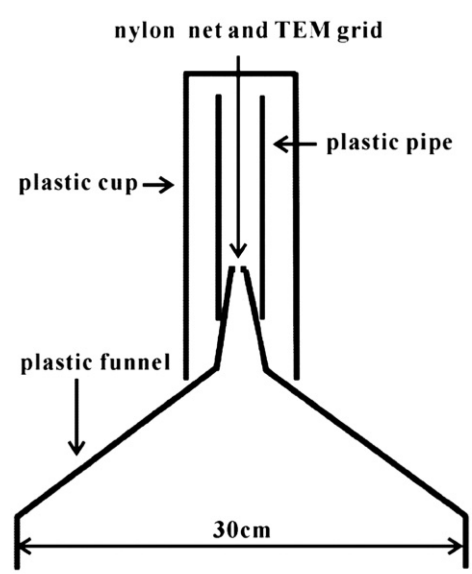

Fig. 2. Sketch of the collector for geogas particles.

sediment samples were collected and placed in 150-ml beakers. 50 ml of high-purity water was added to each. After they were ultrasonically treated for 30 min, a small drop of the solution was dipped onto a copper grid coated with a carbon film for TEM analysis.

4. Results

Under TEM, we found gold particles with irregular shape. EDS analysis revealed that their component is gold. Fig. 3a shows that the size of gold particle is 200 nm × 300 nm. Fig. 3b shows an irregular assemblage made up of gold particles each about 10 nm in diameter. The total size of the assemblage is 150 nm × 300 nm. This is the first time that gold particles have been described in geogas particles by TEM. Fig. 4 shows spherical Hg-bearing particles. The diameters of these particles vary from about 30 nm to 120 nm (mainly from 50 nm to 70 nm). EDS analysis revealed that their main components are Hg (14.93%), S (43.40%), O (26.32%), and Si (9.19%), with minor amounts of Cl (3.39%), and K (2.76%). It can be seen that the smaller Hg-bearing particles were absorbed by greater Hg-bearing particles and the smaller particles formed the chain of spherical particles. Fig. 5 shows two kinds of Pb-bearing particles. Fig. 5a shows spherical Pb-bearing particles with diameters varying from 50 nm to 100 nm. EDS analysis revealed that their main components are Pb (35.74%), N (14.25%), and O (47.02%), with minor amounts of Sn (2.99%). Possibly, the particles are lead nitrates. Fig. 5b shows a cudgel Pb-bearing particle. Its components are Pb (55.88%), S (13.87%), O (26.18%), and Fe (4.08%), suggesting that they may be mainly $PbSO_4$ containing minor amount of $Fe_2(SO_4)_3$. The length of the particle is 200 nm and its width about 35 nm. Fig. 6 shows a Zn- and Sn-bearing particle. EDS analysis revealed that the main components of the ellipsoid particle are Zn (51.36%), Sn (34.61%), and O (7.79%), with minor amounts of Si (1.31%), Br (2.11%), and Fe (2.83%). Fig. 7 shows an assemblage of particles with diameters of 120 nm, which is made up of particles about 20 nm in size. Their components are W (79.13%) and O (20.87%), suggesting that they are WO_3. Electron diffraction pattern indicated that the W-bearing particles are non-crystalline. Fig. 8 shows two kinds of Fe-bearing particles. Fig. 8a shows a needle-shaped Fe-bearing particle. EDS analysis revealed that its main components are Fe (54.36%), O (25.95%), and S (13.35%), with minor amounts of Si (6.34%). Possibly, the needle-shaped particle is ferric sulfate. Fig. 8b shows irregular Fe-bearing particles with sizes ranging from 15 to 40 nm. They were randomly distributed. EDS analysis revealed that their main components are Fe (67.90%), O (30.93%) with minor amounts of S (1.17%), suggesting that they may be mainly Fe_2O_3. Fig. 9 shows a Ca-bearing particle assemblage with a size of 300 nm × 300 nm, which is made up of very fine-sized strip particles. EDS analysis revealed that its main components are Ca (36.84%), O (31.02%), S (27.66%), and Si (4.48%). Fig. 10 shows rhombic plate-shaped particles. EDS analysis revealed that their main components are Ti (59.95%), and O (40.05%), suggesting that they are TiO_2 particles. The sizes of the particles are about 80 nm × 120 nm. On the basis of their characteristics of shapes, which are different from those of rutiles and anatases, the rhombic plate-shaped particles may be identified as brookites. Fig. 11 shows irregular particles. EDS analysis revealed that their main components are Al (52.93%), and O (47.07%), suggesting that they may be Al_2O_3. Fig. 12 shows an Si-bearing hexagonal particle. EDS analysis revealed that the main components are Si (40.73%), O (50.87%) with minor amounts of Fe (4.60%), Ca (1.82%), and Al (1.99%), suggesting that it may be mainly SiO_2. The illite is good-crystalline lath-shaped crystal (Fig. 13) with large ratio of length (250 nm) and width (about 30 nm). EDS

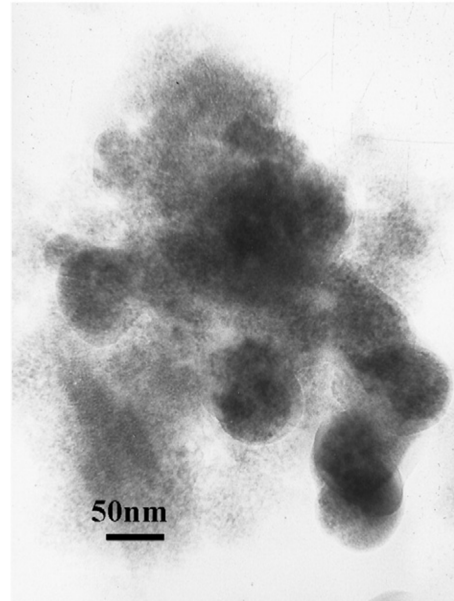

Fig. 4. TEM photomicrograph of Hg-bearing particles.

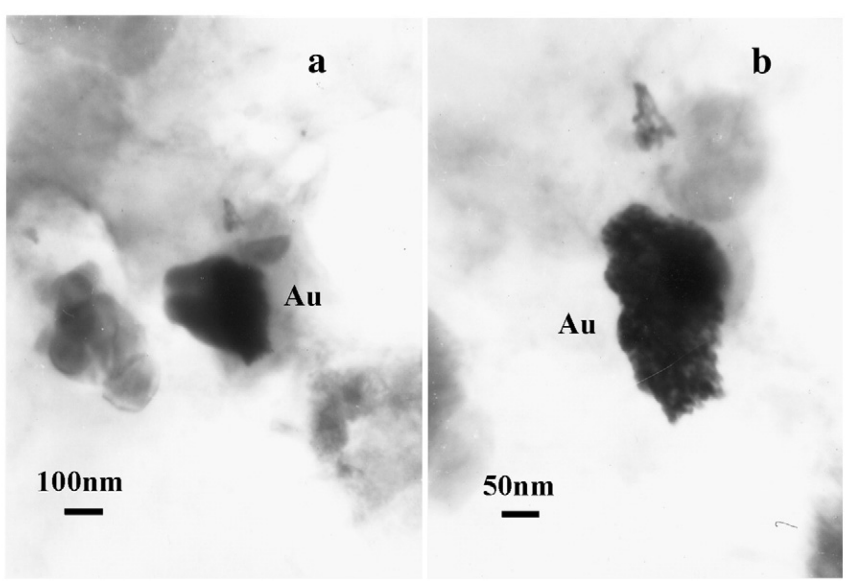

Fig. 3. TEM photomicrograph of (a) gold particle and (b) irregular assemblage made up of gold particles about 10 nm in size.

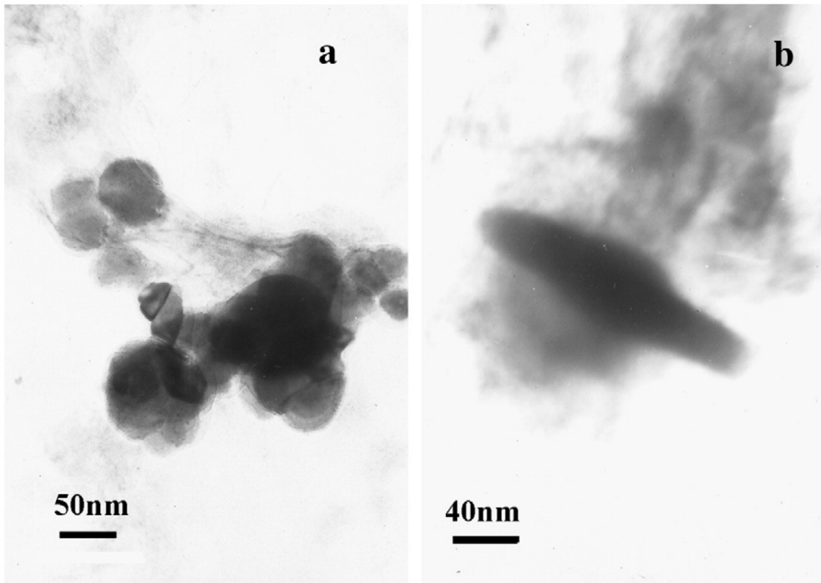

Fig. 5. TEM photomicrograph of (a) spherical Pb-bearing particles and (b) cudgel Pb-bearing particle.

analysis revealed that the compositions of illite are Si (24.93%), Al (15.23%), K (7.58%), Fe (3.58%), Mg (1.13%), and O (45.78%). Under TEM it can be seen that gold particles are associated with Ca-bearing particles. In addition, TEM analyze shows Hg-, Zn-, Sn-, Pb-, or W-bearing particle, and gold particle cannot be found in all blank contrast samples from barren area. Mineral phases in the Quaternary sediments from the ore district are mainly kaolinite, with minor amounts of illite, halloysite, and hematite.

5. Discussion and conclusions

5.1. Origin of the geogas particles

Previous studies have indicated that high concentration (anomaly) of metallogenic elements (such as Au) of the geogas substances is closely related to concealed ore bodies (Malmqvist and Kristiansson, 1984; Kristiansson et al., 1990; Wang et al., 1997; Tong et al., 1998; Xie et al., 1999; Malmqvist et al., 1999). In our work, the Hg-, Zn-, Pb-, or W-bearing particles and gold particles have been not found in blank contrast samples from barren area, showing that the geogas particles are related to concealed ore bodies. They may originate from ore minerals in concealed ore bodies. Hg-bearing particles may originate from cinnabar. Pb-bearing particles may originate from galena; Zn-bearing particles may originate from sphalerite. The high S concentration in some particles may be related to a large number of sulfides in concealed ore bodies. A common feature is that all these Hg-, Zn-, Pb-, or W-bearing particles contain O, suggesting that oxidation may occur before their ascent from the earth's interior to the surface. Possibly, the particles formed during the weathering processes of ores after the period of active mineralization. As the particles in concealed ore deposits interact with ascending gas flows, they are transported to the earth's surface. The content of illites in concealed ore could reach as high as 10% (Du et al., 1993), while the content of illites in the Quaternary sediments is less than 3%. More likely, the illite originates from concealed ore bodies. SiO_2,

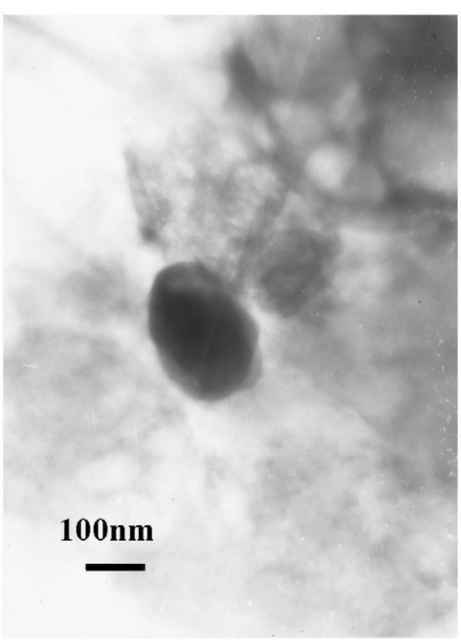

Fig. 6. TEM photomicrograph of Zn- and Sn-bearing particle.

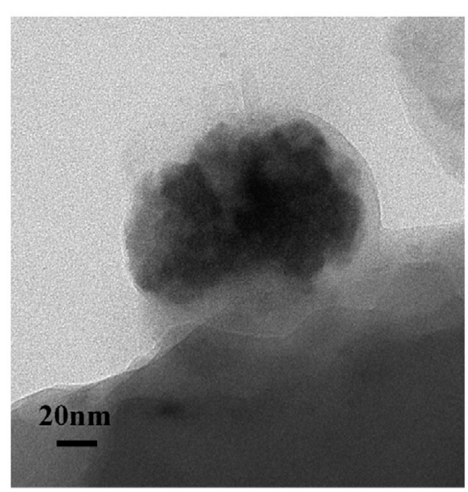

Fig. 7. TEM photomicrograph of W-bearing Particle assemblage.

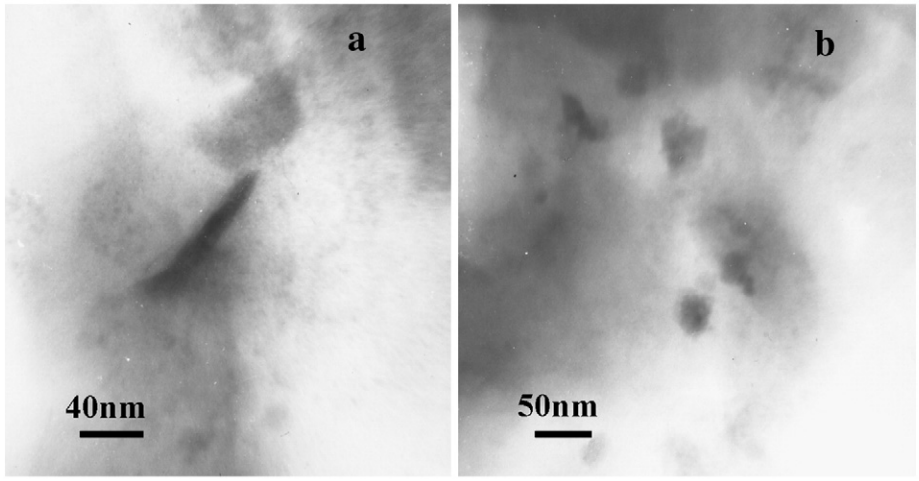

Fig. 8. TEM photomicrograph of (a) needle-shaped Fe-bearing particle and (b) irregular Fe-bearing particles (small black points).

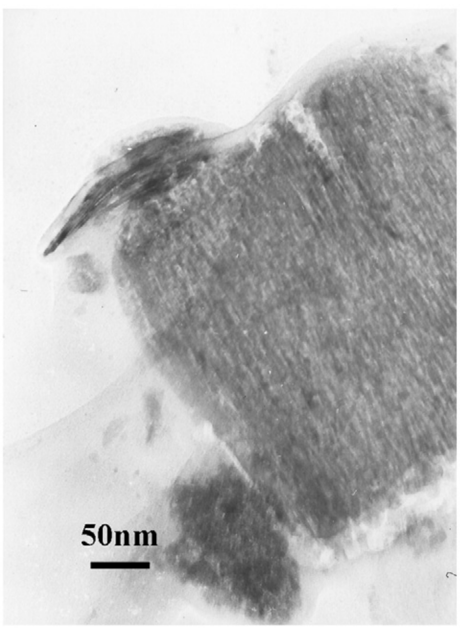

Fig. 9. TEM photomicrograph of Ca-bearing particle assemblage.

TiO_2, and Al_2O_3 particles may originate from the ore bodies and the wall rocks, or Quaternary sediments.

5.2. Implications of the geogas particles

The particle forms and components can provide more direct information of concealed ore bodies than those provided by element concentrations. It is more reliable to certify the existence of concealed ore bodies according to gold particle and Hg-, Zn-, Sn-, Pb-, or W-bearing particle in geogas, because high element concentrations may sometimes caused by other factors besides concealed ore bodies. In addition, we can deduce the mineral composition and the mineral assemblage feature of the concealed ore bodies by particle sizes, shapes, chemical components, and the association among particles in ascending gas flows. The information is very important for mineral exploration. It can be used together with other methods to search for concealed mineral deposits and will develop a new method of mineral exploration with a greater success rate than that of conventional geophysical and/or geochemical methods. Apparently, our research results can also be used to search for other concealed deposits such as lead, zinc, mercury, tungsten, and tin. Au concentration anomalies have been detected in surface geogas associated with oil–gas accumulations (Yang et al., 2000), this study results may apply to exploration for oil–gas accumulations. Literatures have shown that

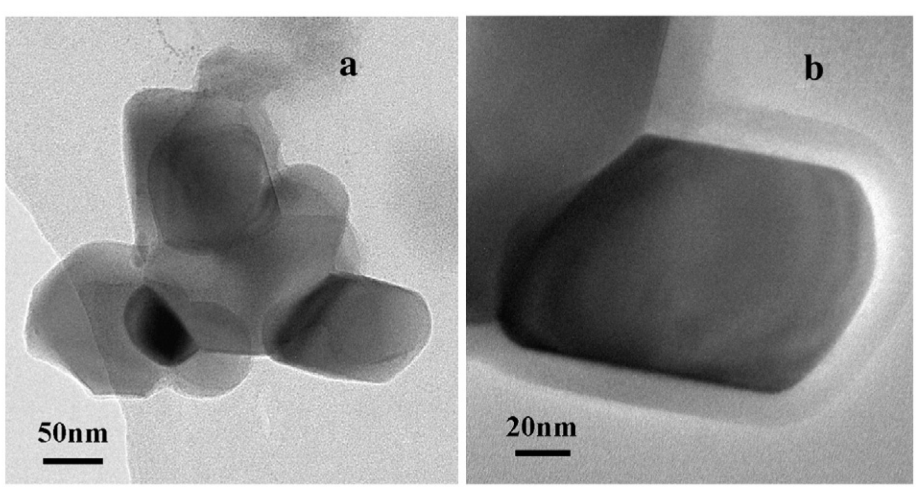

Fig. 10. (a) TEM photomicrograph of TiO_2 particles. (b) An enlargement of the particle at the lower right-hand corner of the left picture.

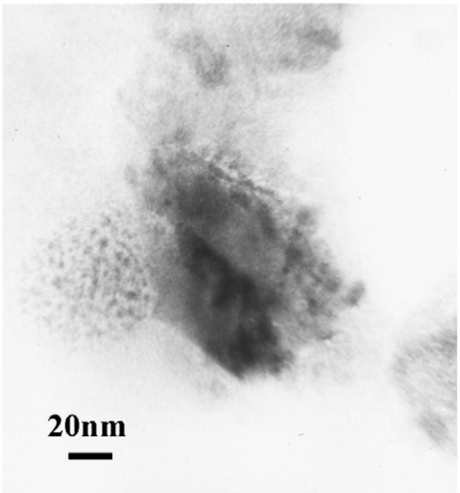

Fig. 11. TEM photomicrograph of Al_2O_3 particle.

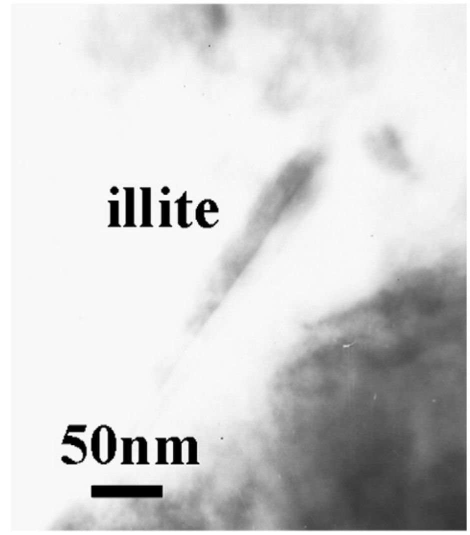

Fig. 13. TEM photomicrograph of illite particle.

concentrations of tungsten, etc. in geogas of the fault related to earthquake are variable (Ge et al., 2000). Geogas particle characteristic of the fault may enhance the accuracy of earthquake prediction. Geogas flows can carry toxic gases or substances (Etiope and Lombardi, 1996; Etiope, 1998; Etiope and Martinelli, 2002; Zhou et al., 2003). Our research methodology may also be used in monitoring the flow of toxic metallic particles from the Earth's interior to the atmosphere. The results show that Pb, W, and Fe can be transported as gas-carried solid WO_3, $PbSO_4$, and Fe_2O_3 particle in the crust. This may enhance geochemical dispersion theory. Moreover, the behavior of gold transport in geological processes has been a controversial subject for several decades. Recently, some researchers suggested that gold could transport as reduced sulfur complexes in the vapor phase of hydrothermal systems at high temperatures and pressures (Pokrovski et al., 2006; Zezin et al., 2007). Other researchers proposed that gold can move as gold particles in ore-forming solution (Zhu and Wang, 2002). The finding of gold particles in geogas indicates that gold can be transported as particle by gas derived from the Earth's interior at temperatures close to room temperature. This may provide a new explanation for geochemistry behavior of gold in crust (e.g. ore-forming process).

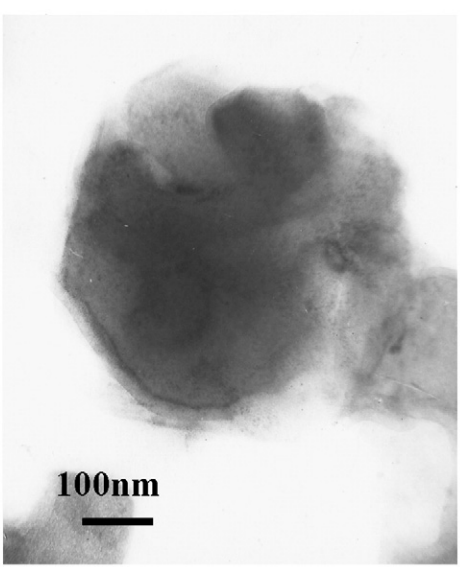

Fig. 12. TEM photomicrograph of SiO_2 particle.

Acknowledgements

Projects 40773037, 40673044 and 40273027 are supported by the National Natural Science Foundation of China. The authors wish to thank Zhao Wenxia, Jiang Dan and Liang Chaolun of the Instrument Analysis Center of the Sun Yat-sen University for assistance in microscopic analysis.

References

Annunziatellis, A., Ciotoli, G., Lombardia, S., Nolasco, F., 2003. Short- and long-term gas hazard: the release of toxic gases in the Alban Hills volcanic area (central Italy). Journal of Geochemical Exploration 77, 93–108.

Cameron, E.M., Hamilton, S.M., Leybourne, M.I., Hall, E.M., McClenaghan, M.B., 2004. Finding deeply buried deposits using geochemistry. Geochemistry: Exploration, Environment, Analysis, 4, 7–32.

Cao, J.J., Liang, Z.R., Liu, K.X., Zhang, K., Peng, Z.L., 2004. Simulation experiment on adsorption of the geogas-carried gold nanoparticles by the weathered crust of red beds. Progress in Natural Science 14, 826–829 (in Chinese).

Du, J.E., Ma, C.H., Zhang, G.H., 1993. Mineralization characteristics of the Changkeng gold-silver deposit, Guangdong province. Guangdong Geology 8, 1–8 (in Chinese with English abstract).

Etiope, G., 1998. Transport of radioactive and toxic matter by gas microbubbles in the ground. Journal of Environmental Radioactivity 40, 11–13.

Etiope, G., Lombardi, S., 1996. Laboratory simulation of geogas microbubble flow. Environmental Geology 27, 226–232.

Etiope, G., Martinelli, G., 2002. Migration of carrier and trace gases in the geosphere: an overview. Physics of the Earth and Planetary Interiors 129, 185–204.

Ge, L.Q., Tong, C.H., Li, J.C., Sheng, S.P., Yang, F.G., 2000. INAA and ATEM study of geogas materials from concealed faults. Trace Microprobe Techniques 18, 51–60.

Gold, T., Soter, S., 1980. The deep earth-gas hypothesis. Scientific American. 242, 132–138.

Hirner, A.V., 1998. Organometal (loid) species in geochemical exploration: preliminary qualitative results. Journal of Geochemical Exploration 64, 133–139.

Kristiansson, K., Malmqvist, L., 1980. A new model mechanism for the transportation of radon through the ground. Society of Exploration Geophysicists Fiftieth Annual International Meeting, Houston, Texas, pp. 2535–2565.

Kristiansson, K., Malmqvist, L., 1982. Evidence for nondiffusive transport of Rn in the ground and a new physical model for the transport. Geophysics 47, 1444–1452.

Kristiansson, K., Malmqvist, L., 1987. Trace elements in the geogas and their relation to bedrock composition. Geoexploration 24, 517–534.

Kristiansson, K., Malmqvist, L., Persson, W., 1990. Geogas prospecting: a new tool in the search for concealed mineralizations. Endeavor (New Series) 14, 28–33.

Liang, H.Y., Xia, P., Wang, X.Z., Cheng, J.P., Zhao, Z.H., Liu, C.Q., 2007. Geology and geochemistry of the adjacent Changkeng gold and Fuwang silver deposits, Guangdong Province, South China. Ore Geology Reviews 31, 304–318.

Malmqvist, L., Kristiansson, K., 1984. Experiment evidence for an ascending micro-flow of geogas in the ground. Earth and Planetary Science Letters 70, 407–416.

Malmqvist, L., Kristiansson, K., Kristiansson, P., 1999. Geogas prospecting—an ideal industrial application of PIXE. Nuclear Instruments and Methods in Physics Research B 150, 484–490.

Mao, X.D., Wu, W.H., Huang, S.J., 2007. Ore types and mineral assemblage of the Changkeng Au–Ag deposit, Guangdong, South China. Journal of Chengdu University of Technology 34, 7–14 (in Chinese with English abstract).
Morner, N.A., Etiope, G., 2002. Carbon degassing from the lithosphere. Global and Planetary Change 33, 185–203.
Pokrovski, G.S., Borisova, A.Y., Harrichoury, J.-C., 2006. The effect of sulfur on vapor–liquid partitioning of metals in hydrothermal systems: an experimental batch-reactor study. Geochimica et Cosmochimica Acta 70, A498.
Sun, X.M., Norman, D.I., Sun, K., Chen, B.H., Chen, J.D., 2003. Organic gases in fluid Inclusions of ore minerals and their constraints on ore genesis: a case study of the Changkeng Au–Ag deposit, Guangdong, China. Acta Geologica Sinica 77, 86–94.
Tong, C.H., Li, J.C., 1999. A new method searching for concealed mineral resources: geogas prospecting based on nuclear analysis and accumulation sampling. Journal of China University of Geosciences 10, 329–332.
Tong, C.H., Li, J.C., Ge, L.Q., Yang, F.G., 1998. Experimental observation of the nano-scale particles in geogas matters and its geological significance. Science in China Series D 41, 325–329.
Wang, X.Q., Cheng, Z.Z., Lu, Y.X., Xu, L., Xie, X.J., 1997. Nanoscale metals in Earthgas and mobile forms of metals in overburden in wide-spaced regional exploration for giant deposits in overburden terrains. Journal of Geochemical Exploration 58, 63–72.
Wang, X.Q., Wen, X.Q., Ye, R., Liu, Z.Y., Sun, B.B., Zhao, S.D., Shi, S.J., Wei, H.L., 2007. Vertical variation and dispersion of elements in arid desert regolith: a case study from the Jinwozi gold deposit, northwestern China. Geochemistry: Exploration, Environment, Analysis 7, 163–171.
Xie, X.J., Wang, X.Q., Xu, L., 1999. Orientation study of strategic deep penetration geochemical methods in the central Kyzylkum desert terrain, Uzbekistan. Journal of Geochemical Exploration 66, 135–143.
Yang, F.G., Tong, C.H., Wang, H.N., Hua, R.M., 2000. Mechanism of geogas substance transportation on oil and gas field. Geochimica 29, 442–446 (in Chinese with English abstract).
Zezin, D.Y., Migdisov, A.A., Williams-Jones, A.E., 2007. The solubility of gold in hydrogen sulfide gas: an experimental study. Geochimica et Cosmochimica Acta 71, 3070–3081.
Zhang, S., Li, T.J., Wang, L.K., 1997. Thermodynamic modelling of ore-forming mechanism of the Changkeng gold–silver deposits in Guangdong Province. Acta Geologica Sinica 71, 433–445.
Zhou, Z.Y., Tao, S., Xu, F.L., Dawson, R., 2003. A physical–mathematical model for the transport of heavy metals and toxic matter from point sources by geogas microbubbles. Ecological Modelling 161, 139–149.
Zhu, X.Q., Wang, Z.G., 2002. Gold occurrence and ore genesis, Yata micro-disseminated gold deposit, Guizhou, Southwest China. Chinese Journal of Geochemistry 21, 370–373.